



Open Archive Toulouse Archive Ouverte (OATAO)

OATAO is an open access repository that collects the work of Toulouse researchers and makes it freely available over the web where possible.

This is an author-deposited version published in: <http://oatao.univ-toulouse.fr/>
Eprints ID : 2540

To link to this article :

URL : <http://dx.doi.org/10.1063/1.2358838>

To cite this version : Dragoman, M. and Muller, A. and Neculoiu, D. and Vasilache, D. and Konstantinidis, G. and Grenier, K. and Dubuc, D. and Bary, L. and Plana, R. and Flahaut, Emmanuel (2006) [*High performance thin film bulk acoustic resonator covered with carbon nanotubes*](#). Applied Physics Letters, vol. 89 . 143122-1-143122-3. ISSN 0003-6951

Any correspondence concerning this service should be sent to the repository administrator: staff-oatao@inp-toulouse.fr

High performance thin film bulk acoustic resonator covered with carbon nanotubes

M. Dragoman,^{a)} A. Muller, D. Neculoiu, and D. Vasilache
*National Research and Development Institute in Microtechnology, Str. Erou Iancu Nicolae 32B,
077190 Bucharest, Romania*

G. Konstantinidis
FORTH-IESL-MRG Heraklion, P.O. Box 1527, Crete 71110, Greece

K. Grenier, D. Dubuc, L. Bary, and R. Plana
LAAS CNRS, 7 Avenue du Colonel Roche, 31077 Toulouse Cedex 4, France

E. Flahaut
*Centre Interuniversitaire de Recherche et d'Ingénierie des Matériaux, UMR CNRS 5085,
Université Paul Sabatier, 31062 Toulouse, France*

This letter presents experimental results concerning a thin film bulk acoustic wave resonator realized on a thin GaN membrane and covered with a thin film of double walled carbon nanotube mixture. The quality factor was measured before and after the coating of the resonator with the nanotube thin film. The quality factor has increased more than ten times when the resonator was coated with nanotubes, due to their high elasticity modulus and low density, which confers a much higher acoustic impedance of the resonator electrodes and thus confines much better the longitudinal acoustic standing waves inside the resonator.

DOI: [10.1063/1.2358838](https://doi.org/10.1063/1.2358838)

The film bulk acoustic wave resonator (FBAWR) consists of a piezoelectric semiconductor thin film sandwiched between two metallic electrodes and excited by a microwave signal. The piezoelectric semiconductor transforms the microwave signal into a longitudinal acoustic standing wave confined between the two electrodes when the microwave signal frequency is equal with the resonator acoustic resonant frequency $f_0 = v_{a,p}/2t$, where $v_{a,p}$ is the acoustic velocity of the piezoelectric semiconductor and t is its thickness. As a result of this resonance phenomenon the FBAWR behaves as a Fabry-Pérot-like cavity. Tuning the microwave frequency around f_0 , the signature of the FBAWR displays a very narrow and deep return loss RL [where $RL = 20 \log(r)$, where r is the reflection coefficient] when the microwave frequency attains the frequency f_0 . The conversion of microwave signals into mechanical vibrations of the resonator can be visualized¹ using laser interferometry with an impressive optical resolution and a speed of 5×10^6 points/h.

Depending on the thickness of the piezoelectric semiconductor which does not exceed a few microns, the FBAWR resonates in the 1–10 GHz range with a quality factor in the range of 200–1000 or even higher and have a very small area of a fraction of a mm². Therefore, FBAWR are miniaturized devices which are very attractive for many applications ranging from wireless communications² up to gas and biological sensors³ due to the high quality factor and their additional mass sensitivity of less than 1 ng/cm².

The piezoelectric semiconductors AlN and ZnO are used frequently for FBAWRs nowadays due to their strong piezoelectricity. However, we have used GaN as a piezoelectric semiconductor, which also has a high piezoelectric coefficient, comparable with that of AlN, (Ref. 4) but can be easily

integrated with Si (Ref. 5) or GaN-based transistors.

In this respect, we have fabricated a GaN thin membrane supported by a Si (111) substrate having a surface of $500 \times 500 \mu\text{m}^2$ and a thickness of 1.8 μm . Further, we have patterned on the membrane a top metallic electrode (Au) with the dimension of $200 \times 200 \mu\text{m}^2$ defining the FBAWR rectangular shape. The backside of the membrane was also metallized with Al to create the FBAWR resonator. The entire technological procedure based on the micromachining techniques, the electromagnetic modeling, and the very first measurements are described in Ref. 6. The GaN FBAWR is displayed in Fig. 1.

The FBAWR electrode material plays a crucial role in the FBAWR performances,⁷ a fact that is not always recognized, although the main role of electrodes is to confine and preserve the longitudinal acoustic standing waves between the facets of the resonator. Reference 7 demonstrates that electrodes with a high acoustic impedance suppress the spurious responses of the FBAWR and produce a significant increase of the quality factor. The acoustic impedance of the

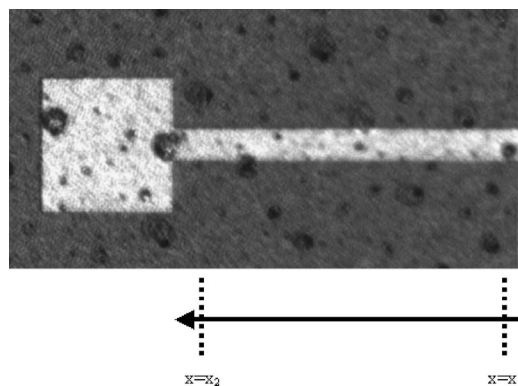


FIG. 1. SEM images of GaN FBAWR. The points x_1 and x_2 are located at, respectively, 400 and 30 μm away from the resonator.

^{a)} Author to whom correspondence should be addressed; electronic mail: mircead@imt.ro and mdragoman@yaoo.com

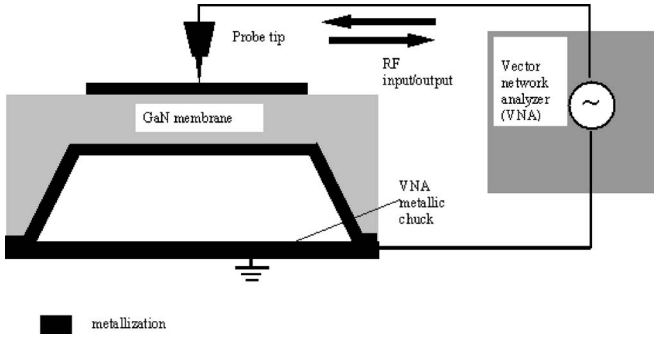


FIG. 2. Setup for FBAWR microwave characterization.

electrodes is $Z_a = v_{a,el} \rho_e = \sqrt{\rho_e E_{el}}$, where $v_{a,el}$ is the sound velocity in the electrodes, E_{el} is the Young modulus of the electrodes, and ρ_e is their density. Moreover, the prerequisites of high- Q FBAWR require from electrodes a low density ρ_e , a high acoustic impedance Z_a (hence a high E_{el}), and a low electrical resistivity.⁷ Usually the electrode materials are Au, Ti, or Pt, which display typically a RL from -12 to -14 dB and a quality factor of 80 – 300 in the case of AlN (see Ref. 7) for the quality factor defined as $Q = f_0/\Delta f_3$ dB. When these electrode materials are replaced with Mo or Ru, a significant improvement of RL (around -24 dB) and an increase of Q with a factor 3 – 4 are observed due to a higher acoustic impedance of the electrodes.⁷

However, the best electrode material of a FBAWR could be a thin film of metallic carbon nanotubes (CNTs) since the CNT displays a low density (1.3 g/cm³), a huge Young modulus (1.2 TPa), which is 15 times greater than that of gold (78 GPa), and a moderate electrical resistivity of 10^{-4} Ω cm. Thus, the main aim of this letter is to coat an existing GaN FBAWR, reported in Ref. 6, with CNTs and to measure the changes in the RL and Q in order to prove that the FBAWR quality factor is significantly enhanced. It should be mentioned that recently⁸ the carbon nanotubes have been used to increase the quality factor of an AT-cut micromachined quartz resonator to about 100% working at 29.4 MHz and it was conjectured that this could be valid for thin film bulk acoustic wave devices such as FBAWR. In this respect, our FBAWR resonator is working at resonance frequencies which are 80 times greater than those reported in Ref. 8.

The GaN FBAWR was characterized using the setup indicated in Fig. 2. A sharp probe tip was attached to a high performance vector network analyzer (VNA) and the entire measurement system was carefully calibrated. Then, the FBAWR was interconnected to the measurement system, as indicated in Fig. 2, and the reflection parameter $|S_{11}|$ was measured at the point $x=x_1$ (see Fig. 1), i.e., near the beginning of the microstrip line located at about 400 μ m away from the resonator. After the FBAWR was measured without any coating, a double wall carbon nanotube (DWCNT) mixture containing about 80% metallic nanotubes was deposited over the FBAWR GaN membrane on both facets. The DWCNTs have an average diameter of 2 nm and an average length of 10 μ m. The debundled DWCNT mixture is immersed in an ethanol solution and mixed via an ultrasonic spinner and deposited over the GaN surfaces with a pipette. After the ethanol evaporation, a uniform deposition of randomly oriented DWCNTs is thus obtained over both facets of the GaN membrane. The technological procedures and the

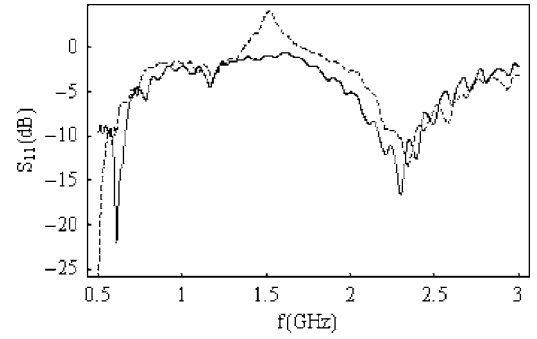


FIG. 3. $|S_{11}|$ parameter of FBAWR (vertical axis in dB) dependence on frequency (horizontal axis in GHz) when the measurement point $x=x_1$, i.e., at a length of about 400 μ m away from the resonator in Fig. 1). The dotted line is assigned for the case of the uncovered resonator, while the solid line corresponds to the case when the resonator was covered with carbon nanotubes.

thorough characterization of DWCNTs used in this experiment are found in Refs. 9–15 demonstrating that we have disposed of very pure DWCNT and with known and verifiable physical properties. Again, the $|S_{11}|$ parameter was measured at the beginning of the microstrip line, which excites the rectangular FBAWR, in almost the same place as in the case when no CNT was deposited on the FBAWR membrane, i.e., at the point $x=x_1$ (see Fig. 1).

The results are displayed in Fig. 3 for both cases, i.e., when the FBAWR membrane (including the electrodes) was initially not covered and then covered with CNTs. A slight lack of calibration is observed in the frequency region out of resonance for the uncovered FBAWR, giving $|S_{11}| > 1$, but this has no influence on the results. This $+4$ dB originates from the fact that the ground of the device was connected to the ground of the VNA via a simple cable since no common ground exists due to the configuration of the FBAWR device. However, the performances of the FBAWR (resonance frequency and return loss) were identical with those previously reported in Ref. 6, measured in different conditions, and therefore we have not further subtracted the cable effect. In Fig. 3 we can see that the microwave response of uncovered and CNT covered resonator are quite modest, i.e., at the resonant frequency of $f_0 = 2.318$ GHz we get a RL around -14 dB and $Q \cong 75$. Moreover, a lot of ripples are observed in both cases indicating a lack of matching. However, as it is pointed out in Ref. 3, it is not necessary to have a high- Q FBAWR to implement a sensitive mass sensor. This can be seen from Fig. 3, where the $|S_{11}|$ curve in the case of the FBAWR covered with CNT is left shifted with about 43 MHz around f_0 , indicating that an additional mass Δm (i.e., CNTs over the top and bottom membrane layers) was added. Based on formulas from Ref. 3 it was determined that the added mass/unit area is $\Delta m = 20.5$ μ g/cm².

Further, we have searched if better results could be obtained by scanning the probe tip along the microstrip line. We have tested several times if reproducible results are obtained by positioning the probe tip with almost the same pressure along the microstrip line at various points then measuring and calibrating the system several times. The results were reproducible but no improvement was observed until we have arrived with the probe at a measurement point located very near the FBAWR resonator, i.e., at the point $x=x_2$ in Fig. 1, i.e., near the end of the microstrip line located at about 30 μ m away from the resonator. Here, suddenly the

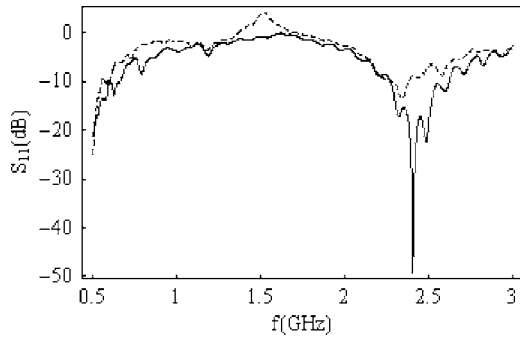


FIG. 4. $|S_{11}|$ parameter of FBAWR (vertical axis in dB) dependence on the frequency (horizontal axis in GHz) when the measurement is performed along the microstrip line near the rectangular resonator (corresponding point $x=x_2$, i.e., at a length of about $30 \mu\text{m}$ away from the resonator in Fig. 1). The dotted line is assigned for the case of the uncovered resonator, while the solid line corresponds to the case when the resonator, was covered with carbon nanotubes.

shape of $|S_{11}|$ was changed dramatically, as indicated in Fig. 4. (Previously, we have also applied the same procedure, when the FBAWR was uncovered with CNTs but the shape of $|S_{11}|$ was unchanged along the microstrip line at any point.)

We can see from Fig. 4 that the RL is now -48 dB, which is an impressive value for a FBAWR indicating that the reflection coefficient is nearly zero, so that an almost perfect matching takes place at the resonant frequency of 2.431 GHz. Moreover, at this frequency the quality factor is around 860, which is a very high value, ten times greater than in the previous situations. The ripples are still observed in the FBAWR response, but the difference between the main sharp response and the second ripple is -28 dB indicating that the resonator is working almost optimally. The question that naturally arises after the examination of Figs. 3 and 4 is why such an important improvement of the FBAWR occurs. One reason is that we have found a matching point between the resonator and the incoming microwave signal, i.e., an optimal feeding point. However, there are many FBAWRs which are perfectly matched but displaying reduced performances compared to that mentioned above. The response is found in the combined action of the nanotubes on the FBAWR membrane. First, the carbon nanotube has improved the acoustical properties of the electrodes increasing their acoustic impedance. This can be seen by calculating the effective elasticity modulus and density of the gold electrodes coated with CNTs. The effective elasticity modulus is $E_{\text{eff}} = (t_e E_e + t_c E_c) / (t_e + t_c)$ and $\rho_{\text{eff}} = (t_e \rho_e + t_c \rho_c) / (t_e + t_c)$, where the subscripts e and c refer to the electrode and coat (CNT), respectively, and t is the corresponding thickness. Considering the typical values for gold density and Young modulus ($\rho_e = 19.3 \text{ g/cm}^3$ and $E_e = 78 \text{ GPa}$) and considering $t_c = 100 \text{ nm}$, we obtain $\rho_{\text{eff}} = 18.6 \text{ g/cm}^3$ and $E_{\text{eff}} = 180 \text{ GPa}$. So, the density is slightly decreasing, while the elastic modulus is increasing with a factor of 2.3. This will double the value of the acoustic impedance of the electrodes. Moreover, as shown in Ref. 1, on the surface of the FBAWR membrane are observed not only useful acoustic standing waves but also traveling waves, which produce energy losses and thus decrease the Q factor. These outrunning waves are strongly attenuated by the deposition of the carbon nanotubes due to their huge stiffness as expressed by their elasticity modulus, which has the highest value among all known materials. The electric input impedance $Z_{\text{in}}(f)$ according to its equation [see

Eq. (12) in Ref. 16] is strongly dependent on the acoustic impedance of the electrodes. Basically, we have tuned these acoustic impedances via a CNT film deposition matching it in one point with that of the VNA generator. However, further simple quantitative considerations cannot be extracted easily based on a simple transmission line model.¹⁶ Here, electromagnetic distributed effects such as standing waves along electrode surfaces are experimentally observed (the ripples around resonant frequency in Figs. 3 and 4), while the electrical permittivity of GaN is quite low ($\epsilon_r = 9.2$ in the range of 1–3 GHz). In these circumstances, a fully electromagnetic model¹⁷ is needed to provide quantitative values and design data applicable to any FBAWR. Such a complex model is presently under study. Simple considerations based on the popular transmission line model of the FBAWR could provide unreliable results. The FBAWR is commonly backed by Bragg-like periodic dielectric structures with the thickness of $\lambda_{a,p}/4$ (where $\lambda_{a,p}$ is the acoustic wavelength), thus forming multilayer acoustic reflector with the role of confining the acoustic waves inside the resonator and realizing a good match. Here, the relation between the input impedance, wavelength, and multilayer thicknesses is straightforward. Such a simple relation does not exist in the case of our device, which shows very good performance due to a simple covering of the FBAWR with a thin layer of carbon nanotubes confining very well the acoustic waves inside the resonator. In conclusion, a high-performance FBAWR based on GaN membrane was demonstrated by covering its membrane with a DWCNT mixture.

The authors acknowledge support through the EU Network of Excellence AMICOM.

- ¹G. G. Fattinger and P. T. Tikka, Appl. Phys. Lett. **79**, 290 (2001).
- ²M. A. Dubois, J. F. Carpentier, P. Vincent, C. Billard, G. Parat, C. Muller, P. Ancey, and P. Conti, IEEE J. Solid-State Circuits **41**, 7 (2006).
- ³H. Zhang and E. S. Kim, J. Microelectromech. Syst. **14**, 699 (2005).
- ⁴L. L. Guy, S. Muensit, and E. M. Goldys, Appl. Phys. Lett. **75**, 4133 (1999).
- ⁵A. Krost and A. Dadgar, Phys. Status Solidi A **194**, 361 (2002).
- ⁶D. Neculoiu, G. Konstantinidis, K. Mutamba, A. Takacs, D. Vasilache, C. Sydlo, T. Kostopoulos, A. Stavrinidis, and A. Muller, 28th IEEE International Semiconductor Conference (CAS), Sinaia, Romania, 3 and 4 October 2005, pp. 119–122.
- ⁷T. Yokoyama, T. Nishihara, S. Taniguchi, M. Iwaki, Y. Satoh, M. Ueda, and T. Miyashita, IEEE Ultrasonics Symposium, Montreal, Canada, 23–27 August 2004, pp. 429–432.
- ⁸A. Goyal, S. Tadigadapa, A. Gupta, and P. C. Eklund, Appl. Phys. Lett. **87**, 204102 (2005).
- ⁹E. Flahaut, R. Bacsa, A. Peigney, and Ch. Laurent, Chem. Commun. (Cambridge) **12**, 1442 (2003).
- ¹⁰E. Flahaut, A. Peigney, Ch. Laurent, and A. Rousset, J. Mater. Chem. **10**, 249 (2000).
- ¹¹S. Osswald, E. Flahaut, H. Ye, and Y. Gogotsi, Chem. Phys. Lett. **402**, 422 (2005).
- ¹²T. Hertel, A. Hagen, V. Talalaev, K. Arnold, F. Henrich, M. Kappes, S. Rosenthal, Ja. McBride, H. Ulbricht, and E. Flahaut, Nano Lett. **5**, 511 (2005).
- ¹³J.-F. Colomer, L. Henrard, E. Flahaut, G. Van Tondeloo, A. A. Lucas, and Ph. Labin, Nano Lett. **3**, 685 (2003).
- ¹⁴M. Sagnes, B. Raquet, B. Lassagne, J. M. Broto, E. Flahaut, Ch. Laurent, Th. Ondarçuhu, F. Carcenac, and Ch. Vieu, Chem. Phys. Lett. **372**, 733 (2003).
- ¹⁵G. Fedorov, B. Lassagne, M. Sagnes, B. Raquet, J. M. Broto, F. Triozon, S. Roche, and E. Flahaut, Phys. Rev. Lett. **94**, 066801 (2005).
- ¹⁶Q. Chen and Q. M. Wang, Appl. Phys. Lett. **86**, 022904 (2005).
- ¹⁷M. Farina and T. Rozzi, IEEE Trans. Microwave Theory Tech. **52**, 2496 (2005).